An investigation of ensemble-based assimilation of satellite altimetry and tide gauge data in storm surge prediction

Paula Etala · Martín Saraceno · Pablo Echevarría

Abstract Cyclogenesis and long-fetched winds along the southeastern coast of South America may lead to floods in populated areas, as the Buenos Aires Province, with important economic and social impacts. A numerical model (SMARA) has already been implemented in the region to forecast storm surges. The propagation time of the surge in such extensive and shallow area allows the detection of anomalies based on observations from several hours up to the order of a day prior to the event. Here, we investigate the impact and potential benefit of storm surge level data assimilation into the SMARA model, with the objective of improving the forecast. In the experiments, the surface wind stress from an ensemble prediction system drives a storm surge model ensemble, based on the operational 2-D depth-averaged SMARA model. A 4-D Local Ensemble Transform Kalman Filter (4D-LETKF) initializes the ensemble in a 6-h cycle, assimilating the very few tide gauge observations available along the northern coast and satellite altimeter data. The sparse coverage of the altimeters is a challenge to data assimilation; however, the 4D-LETKF evolving covariance of the ensemble perturbations provides realistic cross-track analysis increments. Improvements on the forecast ensemble mean show the potential of an effective use of the sparse satellite altimeter and tidal gauges observations in the data assimilation prototype. Furthermore, the effects of the localization scale and of the observational errors of coastal altimetry and tidal gauges in the data assimilation approach are assessed.

Keywords Storm surge prediction · Data assimilation · Ensemble Kalman filter

P. Etala (✉)
Servicio de Hidrografía Naval, Av. Montes de Oca 2124, C1270ABV, City of Buenos Aires, Argentina
e-mail: paulaetala@hidro.gov.ar

M. Saraceno
Centro de Inv. del Mar y la Atmosfera (CIMA)/UBA/FCEN-CONICET, UMI3351-IFAECI/CNRS-CONICET-UBA, Ciudad Universitaria, Pab.II 2 piso, City of Buenos Aires, (1428), Argentina

P. Echevarría
Servicio Meteorológico Nacional, 25 de mayo 658 4 piso, C1002ABN, City of Buenos Aires, Argentina

1 Introduction

The Argentine coast is prone to abnormal sea level rise during particular meteorological events, especially at the highly populated Río de la Plata. Particularly, favourable conditions for surge generation occur on the northernmost shallow section of the shelf next to the mouth of the estuary. Cold outbreaks producing along-shelf sustained strong winds and extratropical cyclones lead to storm surges on the Atlantic coast that propagate into the inner Río de la Plata, and they can occasionally produce flooding in extensive areas. The most severe events occur when intense local winds along the extremely shallow estuary enhance the surge. The densely populated Buenos Aires City (Fig. 1) is affected by storm surges mainly by (1) piling-up estuary waters against the coast (positive surges due to strong southeasterly winds) and thus causing severe floods in the low-lying areas of the city or (2) by partially sweeping
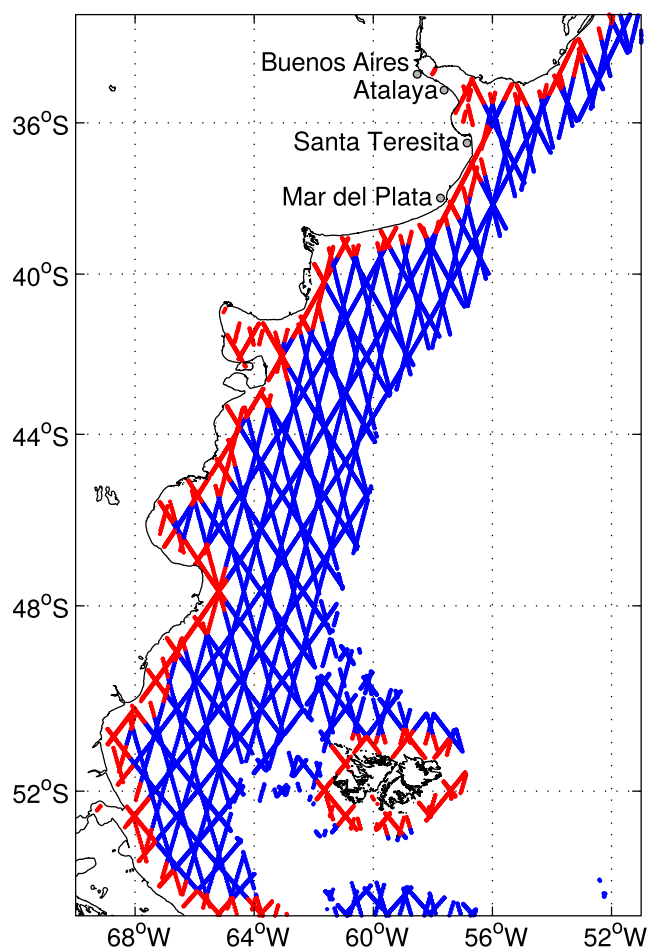
Fig. 1 *Blue* and *red lines* correspond to measurements done by Jason 1, Jason 2 and Envisat during September 2011. *Red lines* are limited to 60 km along-track from the coast. *Blue lines* correspond to other measurements where the water depth is less than 200 m. The positions of the three tide gauges used are indicated with *black dots*, as well as the validation point Buenos Aires

the waters from the coast (negative surges due to strong northwesterly winds), thus affecting navigation safety and drinking water supply. The surge can be anticipated several hours and up to the order of a day ahead by the signal on water level observations at stations conveniently located upstream. The Center for Prevention of the Río de la Plata Rising at the Naval Hydrographic Service, Argentina receives real-time water level data from tide gauges along the Río de la Plata south-western coast and the Atlantic coast, which are shown in Fig. 1. With this information, in conjunction with forecasted winds, the SHN produces advisories which estimate the storm surge with a 12-h lead time that may be increased to 24 h in the case of remote surges generated along the open ocean coasts and detected at Mar del Plata (Fig. 1). Thresholds for a rising sea level warning depend on the position along the coast and vary from 2.10 m

above the reference level at Buenos Aires to 2.00 m at the innermost or delta area. Alerts are issued whenever 2.70 and 2.60 m total water level are expected, respectively. A half-meter rising surge coincident with spring tides can originate a warning. Low water level warnings and alerts are issued for −0.50 and −0.80 m (below the reference level), respectively, from Buenos Aires to the head and into the delta area. In consequence, the relatively long forecast horizon for the innermost zone of the Río de la Plata estuary provides an excellent opportunity to make an attempt to improve the forecast through water level data assimilation.

Sea surface height (SSH) as measured by satellites has become a powerful tool for oceanographic- and climate-related studies. Whereas in the open ocean good accuracy has been achieved, more energetic dynamics and a number of calibration problems have limited applications over continental shelves and near the coast. In recent years, a number of dedicated corrections are suggesting that SSH altimetry data significantly improve coastal altimetry data (Cipollini et al. 2010). Despite the low spatial and temporal coverage of satellite altimetry data, in large regions as the Patagonian shelf, it is expected that they will contribute significantly to the storm surge prediction.

The SMARA numerical model (Etala 2009a) provides guidance to the storm surge forecast at the SHN. Within a collaborative effort of the Argentine Naval Hydrographic Service and the University of Buenos Aires, we aim at investigating the impact and potential benefit of storm surge level data assimilation into the numerical prediction models. The tide gauge observations available only along the northern coast are assimilated jointly with altimeter data on the shelf sea. The sparse cross-track coverage of the altimeters is a challenge to data assimilation. We aim at optimizing their impact by realistically extending the cross-track corrections produced by the observations to the modelled storm surge. We intend to demonstrate that through improved flow-dependent forecast uncertainties from an ensemble in an advanced data assimilation method, we can achieve this goal.

The development of steady-state Kalman filtering (Heemink and Kloosterhuis 1990) for weakly nonlinear 2-D shallow water hydrodynamic models lead to the most extensive application of data assimilation to the storm surge operational prediction (see, e.g. Verlaan et al. (2005)), still in use. Selected tidal gauge observations along the British and Dutch coasts are assimilated to improve the water level forecast at the Royal Netherlands Meteorological Institute (KNMI). The assimilation of remotely sensed data was experimented at an early stage in the application of altimeters to the observation of water level in Philippart et al. (1998). Unfortunately, in a limited area with abundant good quality ground observations like the North Sea, a noticeably impact of satellite altimetry could not be assessed.

Philippart et al. (1998) applied to the fully nonlinear storm surge prediction problem, the Reduced Rank SQuare RooT (RRSQRT) Kalman filter (Verlaan and Heemink 1997), which is an efficient approximation to the Extended Kalman Filter (EKF) through a simplification of the error covariance calculation. The same approach was implemented by Cañizares et al. (1998) in a different 2-D model, also for the North Sea. Both practical methods were later included in a common general framework for data assimilation in hydrodynamic models, the COmmon Set of Tools for the Assimilation of Data (COSTA) (van Velzen and Verlaan 2007), as well as the Ensemble Kalman Filter (EnKF). Other approaches to assimilate data for storm-surge operational prediction considered adjoint techniques (Li et al. 2013; Lionello et al. 2006) and variational data assimilation (Peng and Xie 2006).

Since Evensen (1994) first proposed the EnKF as an alternative to the EKF, where flow-dependent background errors were based on an ensemble, several approaches to the model update or analysis step have been introduced and applied to multiple problems in geophysics. The EnKF algorithm is naturally independent from the prediction model used. An efficient square root EnKF scheme based on the singular evolutive interpolated Kalman (SEIK) filter was implemented by Butler et al. (2012) to the problem of the storm surge produced by hurricanes. The authors succeeded in achieving improved maximum water levels by using uncertainties from hindcasts of an advanced 2-D storm surge model for selected events. Ott et al. (2004) proved the feasibility of an entirely local scheme for the EnKF in the so-called Local Ensemble Kalman Filter (LEKF) and Hunt et al. (2007) dramatically improved the efficiency of calculations in the Local Ensemble Transform Kalman Filter (LETKF). The latter belongs to the SQuare RooT (SQRT) filters type or "deterministic" EnKF, in which an analysis for the ensemble mean is first produced and then the ensemble perturbations expanded through the analysis covariance. To our knowledge, this method has not been applied so far to the storm surge prediction problem and its potential performance is explored through the prototype presented in this work.

The main goal of this initiative is to investigate the feasibility and potential benefit of assimilating observations with storm surge prediction purposes in a context of a large area of generation lacking real-time conventional data, given the opportunity provided by newly available satellite observation techniques. Section 2 refers to the observational data used for both assimilation and validation. In Section 3, we briefly explain the basics of the data assimilation method and describe the application of the Miyoshi and Yamane (2007) implementation of the 4D-LETKF. The data assimilation scheme is mainly focused on a deterministic-type 6-h forecast, represented in this case by the ensemble mean.

Section 4 presents the design of 1-month assimilation experiments. Results are presented and discussed in Section 5. Finally, conclusions are summarized in Section 6.

2 The storm surge observations

Satellite altimetry data have been downloaded using Radar Altimeter Database System (RADS, http://rads.tudelft.nl). The data base contains validated and verified altimeter data products that are consistent in accuracy, format, correction and reference system parameters. Much effort has been put in calibrating and validating the raw data, i.e. harmonization of geophysical corrections, of secondary data and of the measurements themselves. The validation includes editing, tide experiments, radiometer-model collocation and Rossby and Kelvin waves propagation analysis (Naeije et al. 2000). Data for all satellite missions available for the periods of time studied have been included in this study (Fig. 1).

Coastal water level stations are available from the SHN for the northernmost part of the shelf and in the Río de la Plata only. In this study, hourly water level residuals from three tide gauges are used in the assimilation: Mar del Plata at the open sea coast, Santa Teresita at the mouth of the estuary and Atalaya at the mid-estuary (Fig 1). The last two are also used for validation of the 6-h forecasts produced in this work. Satellite altimetry provides some coverage off-shore and, occasionally, on the extensive areas lacking coastal data.

3 The data assimilation method

A basic assumption is that the actual errors-of-the-day lie within a lower dimension space than the full system. Then, if the ensemble system provides a reasonably good estimation of these errors, the dimension of the problem can be reduced locally. The general approach of the EnKF combines the flow-dependent background errors provided by an ensemble prediction and the observations to build the analysis ensemble, including the analysis uncertainty. The analysis ensemble so obtained provides the initial state to a new ensemble forecast cycle. Due to the unavoidable presence of model errors and non linearities, short cycles are in general more suitable to the EnKF, and in particular to the LETKF, than a longer assimilation cycle (e.g. Kalnay et al. 2007)

The 4D-LETKF, as originally coded by T. Miyoshi (Miyoshi and Yamane 2007), has been adapted to assimilate storm surge data into an ad hoc 20-member storm surge model ensemble. This 4-D scheme initializes the ensemble in a 6-h cycle (Fig. 2). Given an n-dimensional model state x and an m-member model ensemble, δX is the $m \times n$
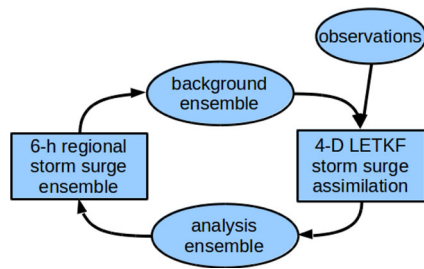
Fig. 2 The 4D-LETKF assimilation cycle. The ensemble forecast provides a first-guess that is corrected with the observations in the analysis. These analysis ensemble members are the initial fields in the next forecast cycle

matrix containing the m perturbations of the ensemble. The i^{st} member perturbation is defined as its departure from the ensemble mean $\delta x_i = x_i - \bar{x}$. We will denote vectors in lowercase and matrices in uppercase.

3.1 The forecast step

The ensemble forecast step is common to any EnKF. It is performed globally in the model space by integrating the model M forward from the analysed state X^a at the time step $t - 1$:

$$X_t^f = M(X_{t-1}^a) \tag{1}$$

Then, the forecast error covariance matrix provided by the ensemble is

$$P^f \approx (m - 1)^{-1} \delta X^f (\delta X^f)^T \tag{2}$$

The SMARA model is a regional 2-D depth-averaged hydrodynamic model used to represent a limited number of tidal constituents and surge, that is extensively described in Etala (2009a). Its one-third degree lat/lon resolution on the shelf is low, when compared to other current deterministic prediction models. In spite of its basic approach and coarseness, the SMARA model showed up to be comparable to global models with assimilation when validated with off-shore altimeter data (Saraceno et al. 2010). Although coastal tidal ranges at the southern shelf are sub-estimated, its behaviour is well balanced throughout the Atlantic coast and the shelf. Its low cost in an ensemble scheme also makes it suitable for this study.

The observation operator H applied to the model variable in the ensemble provides the "model observation", i.e. the model in the observation space $Y^f = H(X^f)$. To get the modelled surge values X^f, water levels from the tides-only model run are substracted from the run including atmospheric forcing and tides. $\delta Y^f = H(\delta X^f)$ is the perturbation of the model observation to the ensemble mean.

3.2 The analysis step: LETKF

The p available observations y^o introduce the new information in the observational increment or innovation in $(y^o - y_i^f)$. The observed water level residuals, calculated as the total observed water level minus the astronomic tide, are considered as the observed surge y^o. The way these observations are considered in the analysis step to update the background (Section 3.2) is what distinguishes LETKF from other EnKF methods.

The LETKF determines the analysis ensemble locally in the space spanned by the ensemble, as a linear combination of the background perturbations. The local transformation formulated by (Hunt et al. 2007) allows to assimilate observations simultaneously and independently from point to point while keeping horizontal smoothness. The updated model state becomes:

$$X^a = \bar{x}^f + (\delta X^f) W^a \tag{3}$$

where W is a base of the space spanned by the perturbations of the ensemble and defined with a null ensemble mean $\bar{w}^f = 0$ and covariance $\tilde{P}^f = (k - 1)^{-1} I$. The authors demonstrate that the solution for W also minimizes the original analysis cost function, and analysis equations analogous to EnKF are solved for the w ensemble in the local $m \times m$ ensemble space, substantially simplified by the variable transformation. Variables in the local space are hereinafter denoted by tilde.

$$\tilde{P}^a = [(m - 1)I + (\delta Y^f)^T R^{-1} (\delta Y^f)]^{-1} \tag{4}$$

where R is the observational error covariance matrix of the locally used observations and the "model observation" y_i^f was defined in Section 3.1. The uppercase in Eqs. 5 and 4 indicates the p observations $\times$ m ensemble members arrange. Finally, $\tilde{P}^a$ is the analysis ensemble perturbation covariance matrix P in the local space, and R is the observational error covariance matrix. The modification to R introduced by the observation localization (10) is described in Section 3.3.

The LETKF belongs to the class of the so-called "deterministic" or square-root EnKF. It updates in a single step the ensemble mean (5) and retrieves the analysis ensemble perturbations from the covariance matrix in Eq. 6. So,

$$\bar{w}^a = \tilde{P}^a (\delta Y^f)^T R^{-1} (y^o - \bar{y}^f) \tag{5}$$

and

$$\delta W^a = [(m - 1) \tilde{P}^a]^{1/2} \tag{6}$$

provide the transformation weights w. The innovation $(y^o - y^f)$ represents the new information provided by the observation with respect to the model state. In Eq. 5, it is

expressed in terms of the perturbation from the ensemble mean.

Equations 4 to 6 are those actually solved by the algorithm in the local space of the ensemble. The full analysis ensemble is then built through (3) back into the global model space. Alternatively, we may choose to update the analysis mean or the deterministic model in a hybrid-type approach by

$$\bar{x}^a = \bar{x}^f + (\delta X^f)\bar{w}^a \tag{7}$$

The analysis ensemble perturbations in this scheme are close to the original background ensemble perturbations, as

$$\delta X^a = (\delta X^f)(\delta W^a) \tag{8}$$

from Eqs. 3 and 7.

The full analysis ensemble is then built including additive inflation, which is a tuning parameter for the ensemble spread, as

$$X^a = \bar{x}^a + (\delta X^a) + AI \times (\delta X^k) \tag{9}$$

where AI is a tuning factor and (δX^k) are the perturbations of an arbitrary ensemble. It is an usual practice to set any linear combination of the forecast perturbations after the spin-up of the assimilation, while additive perturbations may be generated by any other method or randomly at the initiation of the cycles. The particular implementation in this work is detailed in Section 4.

3.3 Observation localization

Any corrections introduced by the observations only take place in the scale of the ensemble perturbations covariance and cross-covariance, as will be shown in Section 5. Either the extent of the ensemble perturbation covariances or an arbitrary localization scale may limit the influence of the observations in space and time in the analysis. Nevertheless, some localization in space and time is required to override occasional spurious background perturbations covariance, not related to the local background uncertainty. Due to the potentially large scale of the surge phenomena, observations within a wide local patch are selected for the analysis around a grid point. The so-called "observation localization" approach is applied, in which the observational error is exponentially increased with distance to the analysis grid point by the function ω in Eq. 10.

$$\omega_{(dist)} = e^{-dist^2/2L^2} \tag{10}$$

The weight factor ω is applied to the inverse R matrix in the calculations. In the local analysis of Eqs. 4 to 6, ω is an attribute of every observation. This "smoothed localization" approach lowers the influence of an observation

to half its value at a distance L while decreasing exponentially. L is called the "localization scale". Although in a classical EnKF approach, as discussed in (Miyoshi and Yamane 2007), the impact of this scale is closely related to the observational errors and smoother than covariance localization, in this LETKF scheme, it impacts directly on the weight of the individual innovation through R in Eq. 5.

Asynchronous observations from altimeters and hourly observations from tide gauges are disposed at hourly time slots within a 6-h assimilation window, centered on the analysis time. The innovations calculated on an hourly basis pair with evolving forecast error covariances in Eq.5. A localization in time $\omega_{(t)}$, completely analogous to Eq. 10, limits the observation influence within the assimilation window, where a parameter T plays the role of the localization scale.

4 Experiments setup

Data assimilation experiments of storm surge observations were carried out on the Argentine continental shelf for September 2011. The experiments on the current prototype were aimed at the assessment of the benefit of data assimilation on the storm surge short-term prediction. We explore the role of the basic parameters in the scheme, such as localization scales and observational errors, in such an impact. The period of study was chosen due to three moderate to strong rising surge events that took place on the northern shelf and estuary in that month. Residuals from hourly water level observations at tide gauges in Fig. 1 are plotted in Fig. 3. The observation in the City of Buenos Aires, at the head of the estuary, is also shown for reference, although it is not included in this study. It will be shown below that the prototype ensemble mean failed to predict accurately the peaks, providing a favourable scenario to test a potential improvement through the assimilation.

Coastal stations are conveniently located for the followup of the storm surge into the Río de la Plata. On the other hand, the lack of data on the rest of the shelf is only tempered by the sparse and unevenly distributed altimeter observations. Typical spatial distributions of data within a 9-h assimilation window are seen in Figs. 6 and 8. This is why the knowledge of the forecast uncertainties becomes particularly important for the correct estimation of analysis increments. Occasionally, covariance of the surge level perturbations $\overline{\delta x_i \delta x_j}$ extends along the coastline. The alongshore storm surge produced by long-fetched southerly winds provides the most suitable scenario for the data assimilation. Alternatively, local southwesterly winds produced by relatively small size perturbations may only benefit from local data. The horizontal scale of the uncertainties and

Fig. 3 Observed storm surge level at Mar del Plata, Santa Teresita, Atalaya and Buenos Aires tide gauges for September 2011
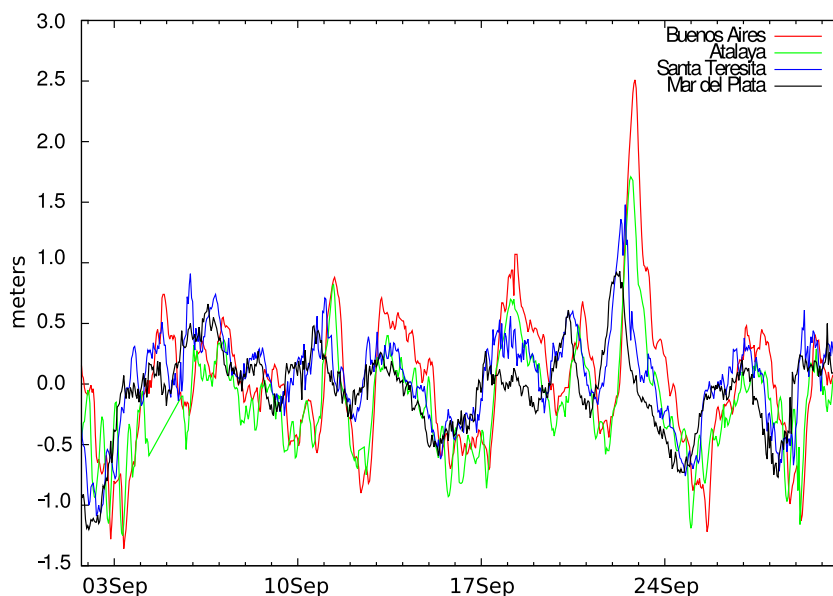
their covariance is clearly reflected in the ensemble mean analysis increments on a case-by-case basis in next section.

The storm surge model ensemble is driven by the NOAA Global Ensemble Forecast System (GEFS) (Wei et al. 2008), obtained from the THORPEX Interactive Grand Global Ensemble (TIGGE) at a 1° × 1° resolution. A major limitation is the too coarse resolution of the atmospheric input for the problem of the storm surge, and possibly a low number of members. We have not investigated into a better estimation of the forecast uncertainties and this is a pending issue. Calibration of an actual system is out of the scope of this work.

The 4D-LETKF initializes the storm surge ensemble members at every cycle. The means provided by the LETKF to act on the ensemble spread is the inflation of the initial state perturbations in Eq. 9 in every cycle. In the spin-up period (2−3 days, not shown) an extra ensemble inflated the spread, which was null at the initial state. That extra ensemble consisted of randomly selected members of the original background ensemble from various time slots within the assimilation window. Inflation at later cycles was handled with additional perturbations from the model ensemble itself, being mindful of the 24-h continuity cycle of the forcing ensemble perturbations so not to introduce extra noise (H. Alves, personal communication). The latter is not a desirable property in our short-cycle system, and any other method of inflation involving the forcing fields perturbations was not considered.

We designed a 9-h $[t − 5, t + 3]$ assimilation window for observations. Data from the tidal gauge network, at least, is usually expected before the initiation of the actual run in an idealized practice. In consequence, the cut-off time for data in wet models may be later that its counterpart for the atmospheric model assimilation cycle. It is true that, in this scenario, observations from hours $[t + 1, t + 3]$ may be assimilated twice, but that would happen in different cycles to different background fields.

The horizontal localization scale L in Eq. 10 ranged from 1000 to 100 km, while the time localization scale T varied between $t ± 3$ and $t ± 1$ hours in our various experiments. The observations get their errors increased according to Eq. 10. Apart from that, the filter performs a gross quality check against first guess before the analysis. We intervened in that control with a preliminary solution, by allowing a tolerance parameterized as a 30 % above the background root mean square error (RMSE) and the observational error, according to the source. We assumed 11- and 5-cm RMSE for the altimeter observational errors in separate tests, and a 3-cm RMSE for the tidal gauge observations. In all cases, we considered the 6-h forecast (background) error against observations as an objective decision criteria.

5 Results and discussion

It is widely known that the spread provided by the atmospheric perturbations only does not explain the magnitude of the errors in the water level forecast. In the context of data assimilation, this would lead to an overweighting of the background fields relative to the observations, due to the underestimation of forecast and model uncertainties. In a recent study, Altaf et al. (2014) discuss the role of covariance inflation in various ensemble Kalman filter methods,
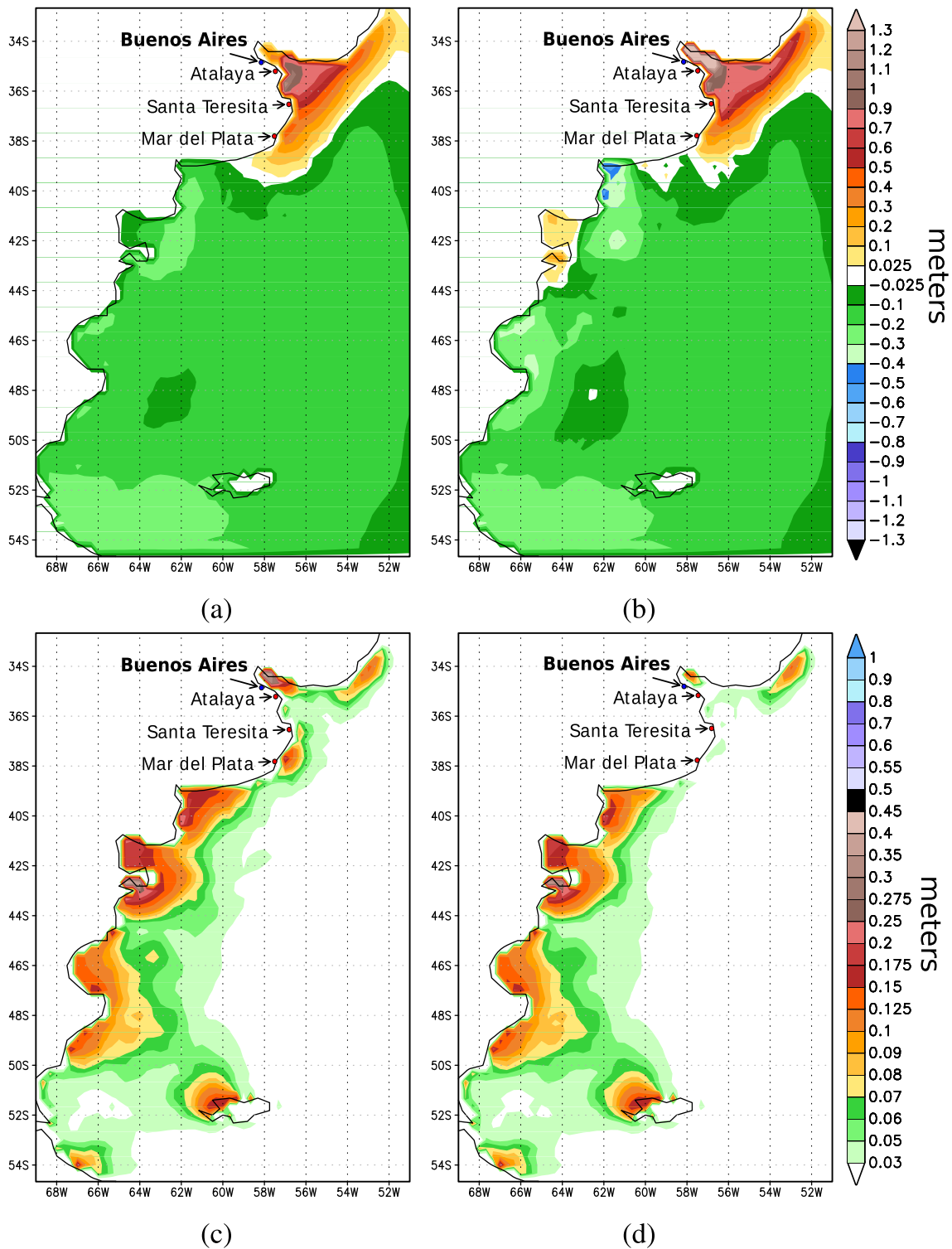
Fig. 4 Background and analysis ensemble mean and spread for the peak of the event in the estuary on 22 September 18:00 from the run with inflated spread, L=500 km, T=1 h, all data used.

Background ensemble mean **(a)**, analysis ensemble mean **(b)**, background ensemble spread **(c)** and analysis ensemble spread **(d)**

applied to storm surge assimilation for practical forecasting purposes. The authors conclude that the use of inflation is effective in a better estimation of the system variance, and it improves the performance of the assimilation, in particular when the ensemble size is small and model errors are not considered.

As mentioned in the previous section, the limitation to capture actual sources of uncertainty has not been comprehensively addressed in this work. We artificially modified the spread by inflating the initial perturbations of the analysis ensemble in various tests, so to roughly match the RMSE from the hindcast to the 12-h forecast storm surge level. For the month of our study, the deterministic SMARA model RMSE in Mar del Plata for those ranges was in the order of 0.15 m. The analysis and background ensemble mean and spread so obtained at the time of the peak of the surge in Buenos Aires are presented in Fig. 4.

The error in the background ensemble mean, i.e. the 6-h forecast after the assimilation evaluates the performance of the data assimilation scheme. The improved initialization should lead to a measurable benefit in the forecast from cycle to cycle. In the following plots in this section, we present the partial effect of different factors we assessed in the scheme. Finally, we present the integral impact of the data assimilation by comparing the same error curves to a control run without data assimilation.

We provide first an overlook on the relative effect of the model confidence against the two sources of observations and their observational errors. In Fig. 5, we test the impact of the calibration of the forecast uncertainties through the analysis perturbations, against the effect of including the altimeter observations. The mean and standard deviation of the forecast error in three different runs for the last 20

Fig. 5 Mean *(upper)* and standard deviation of the error *(lower panel)* of the 6-h forecast ensemble mean versus observations from 10 to 30 September 2011. The *black line* represents the run with all observations. Only tide gauge observations run in *green* and the *red line* denotes the errors for the run with all data when the initial spread is enhanced by additive inflation at every cycle
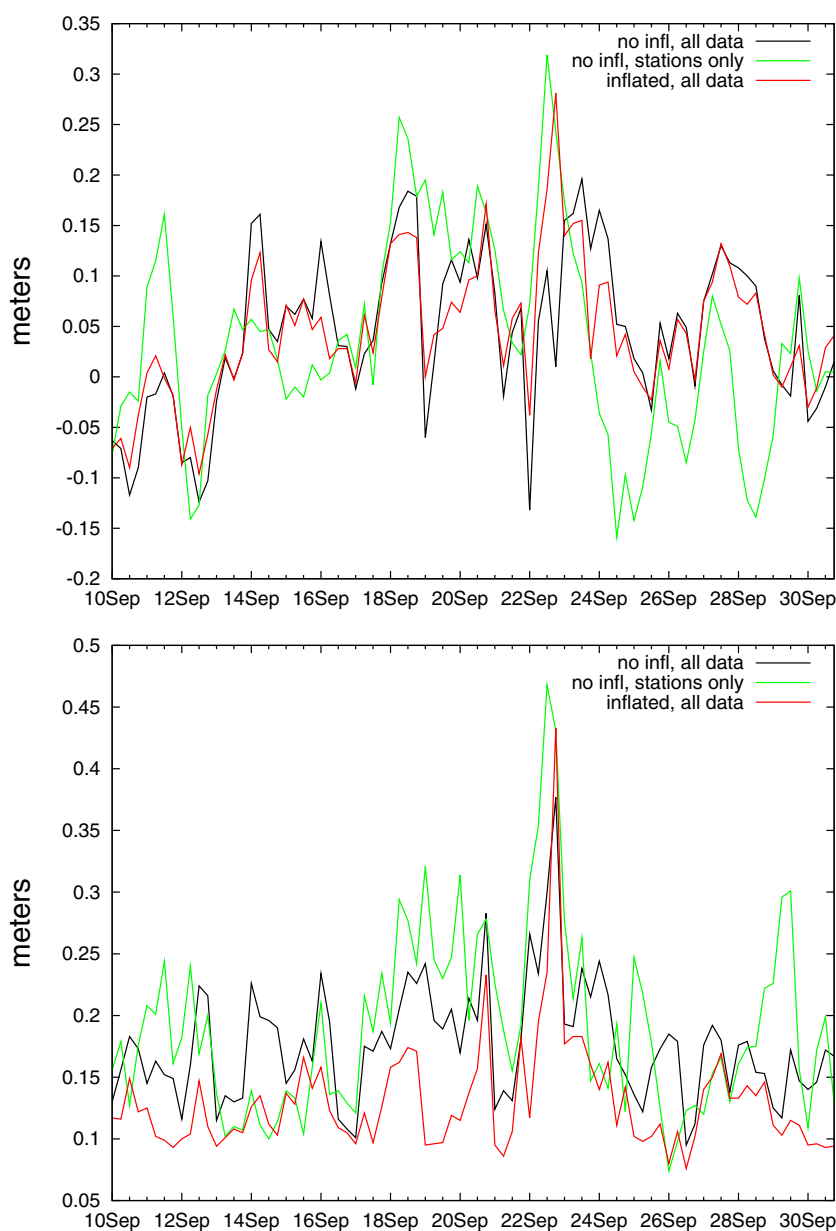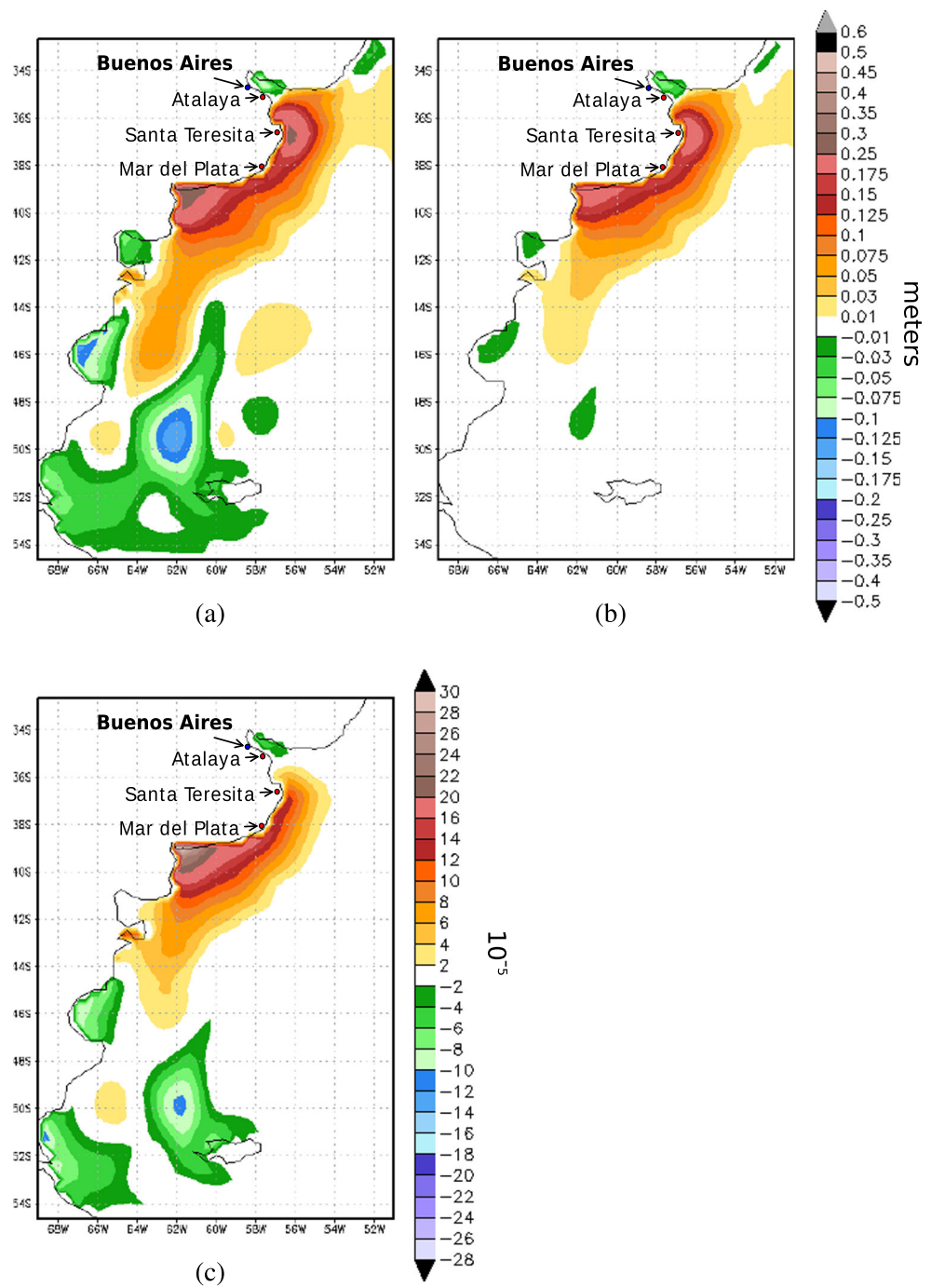
Fig. 6 Upper panels: Storm surge increment (m) in the ensemble mean due to the assimilation of tidal gauges on 7 September 00:00; L=1000 km **(a)**, L=500 km **(b)**. Lower panel **(c)**: Surge level perturbation covariance for Mar del Plata's location at that time $1/(m-1)(\delta X^f)_{MdP}(\delta X^f)$ (units $10^{-5}m^2$). Tidal gauges locations are shown

(a)

(b)

(c)

days of the month are shown in the upper and lower panels, respectively. The red lines in the plots represent the run with inflated perturbations. The black and green lines denote the runs where the model accuracy has been overestimated by not inflating the spread. Black and green differ in the observation sources considered, i.e., black includes altimeters and the run in green has included ground observations only. While the run in red (calibrated spread) generally shows the best performance, we note that the magnitude of

the improvement in the errors is roughly comparable to the inclusion of altimeter observations. Only around the time of the peak (see Fig. 4), including the altimeter data and relying on the model produced the best solution. The latter suggests that overweighting the observations against the background may be dangerous in the case of any misleading data from the very few tidal gauges. The obvious relevance of a comprehensive review of quality control in this approach is, anyway, highlighted.
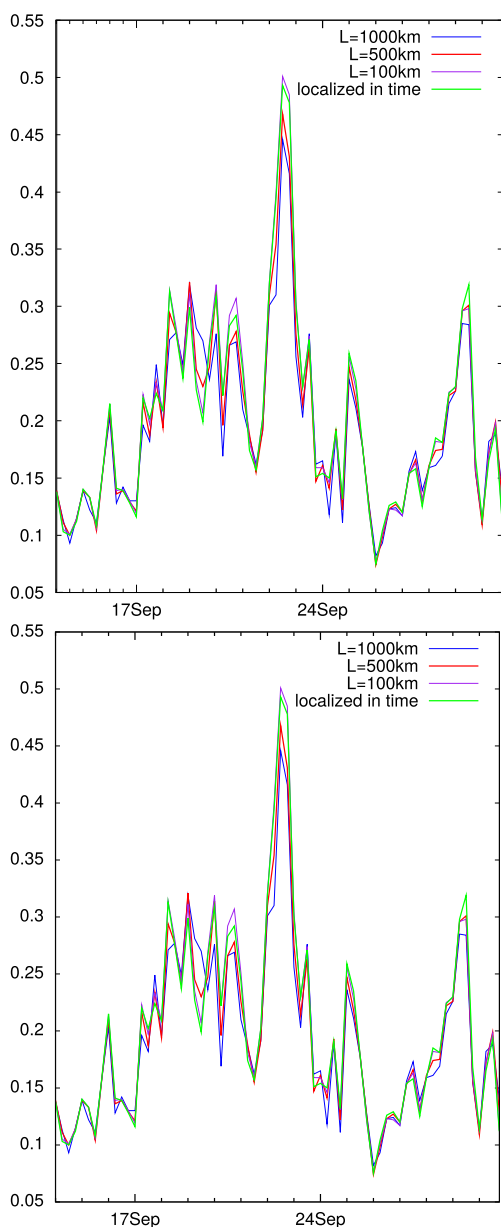
Fig. 7 Mean *(upper)* and standard deviation of the error *(lower panel)* of the 6-h forecast ensemble mean versus observations for the most active period in September 2011. Results correspond to different localization scales for tide gauge observations only

As mentioned in the previous section, the information provided by coastal tide gauges is the key to the storm surge prediction in the estuary. With illustration purposes, the isolated effect of these data on the analysis increments (analysis corrections to the first-guess field) in the ensemble mean is shown in Fig. 6, together with the column of the background ensemble perturbation covariances corresponding to the southernmost station's location (Mar del Plata). In order to avoid any external intervention in the free evolution of covariances of the scheme, values in Fig. 6c correspond
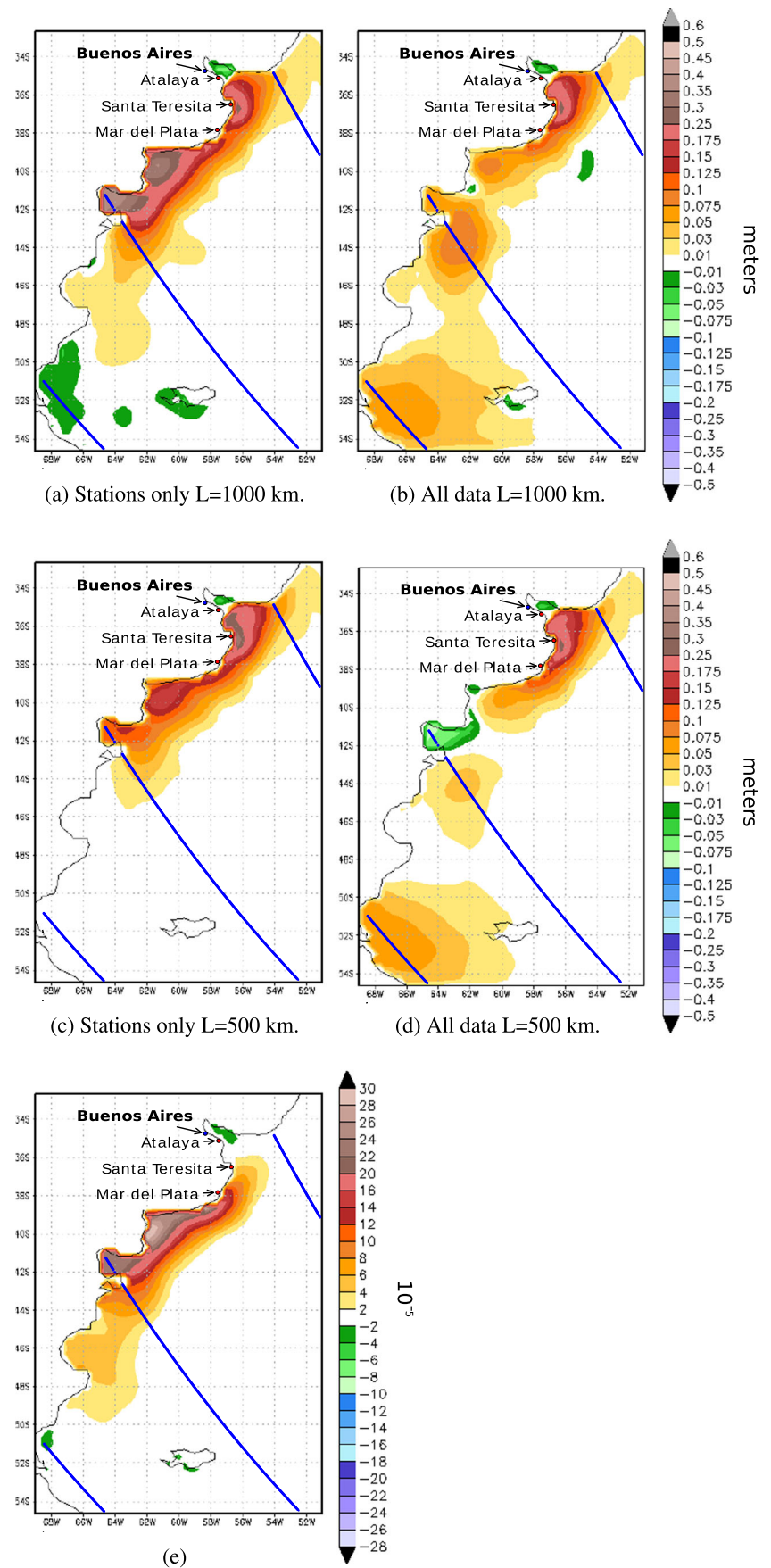
to the run without additional inflation (the lower order of magnitude is noted). Localization scale is L=1000 km and L=500 km for Fig. 6a and b, respectively. Corrections at the southern shelf area in Fig. 6a are based only on the information provided by northern tide gauges and occasional error covariance. These corrections could not be assessed by the inclusion of altimeter observations in the more localized scheme (not shown). Corrections introduced by the altimeters have eventually confirmed that covariances throughout the shelf were realistic, but those cases have been more the exception than the rule in these experiments.

The experiment results in terms of the bias and standard deviation of the errors are presented in Fig. 7. As expected, differences in performance were only noticeably in coincidence with the most significant events. In most cases, the widest localization performed better. An extra time localization to favor the consideration of hourly data did not introduce any benefit.

With the inclusion of altimeter data, differences are even less remarkable in terms of forecast error, but in the same sense as for the stations-only case. Contrast is certainly smoothed when large amounts of satellite data in less perturbed areas are taken into account. We illustrate in Fig. 8 the impact of altimeters on analysis increments during the rising stage of the strongest surge event on 22 September 06:00. Satellite tracks for the assimilation window and tidal gauge locations are also plotted in the figure. Buenos Aires is not assimilated. Corrections above 25 cm in the analysed storm surge at the mouth of the estuary lead to significant water level variations when propagated into the estuary by the forecast, as seen from the validation in Fig. 9 below. Panels Fig. 8a and c show the analysis increments produced by stations only, while, in Fig. 8b and d, altimeters have also been included. In the upper panels Fig.8a and b, a localization scale of 1000 km has been used in the analysis while, in Fig. 8c and d, L=500 km. We note the more realistic increments in panels Fig. 8c and d. The column of the background ensemble perturbation covariance matrix at Mar del Plata's location is displayed in Fig. 8e for reference. Same as Fig. 6c, the covariances do not include additional inflation. The 500-km localization scale looks qualitatively more convenient whenever observations may be more sparse or not available at all, as it is the case in plots on the left. The same conclusion stands for those cases with smaller scale perturbations, as the one shown in Fig. 6. The use of smaller observational errors, as described in Section 3.3, enhanced the local influence of observations (not shown). In all plots on the right, the altimeters correct the exaggerated influence of the isolated tidal gauge stations (Fig. 8a, c) and provide further information in areas lacking coastal observations.

Finally, the mean observational departure of the 3, 4, and 5-h ensemble forecasts is plotted in Fig. 9 for the

Fig. 8 Storm surge increment (m) in the ensemble mean due to the assimilation during the rising storm surge event on 22 September 06:00. L=1000 km in upper panels (**a, b**) and L=500 km in central panels (**c, d**). Experiments in left panels (**a, c**) considered only tide gauge data while panels on the right (**b, d**) include all data in the assimilation. In panel (**e**), surge level perturbation covariance for Mar del Plata's location at that time $1/(m-1)(\delta X^f)_{MdP}(\delta X^f)$ (units $10^{-5}m^2$)

(a) Stations only L=1000 km.

(b) All data L=1000 km.

(c) Stations only L=500 km.

(d) All data L=500 km.

(e)

32 cycles (4 per day), corresponding to the most active week from 17 to 24 September. Only observations from Santa Teresita and Atalaya, at the mouth and middle estuary, respectively, were used in this validation. The benefit introduced by the assimilation is clearly noted in the contrast between the non-assimilation control run (black line) and any other test. Bias is practically bounded to ±0.10 m whenever data assimilation is performed. Experiments varying the localization scale (L) and the altimeters observation error (RMSE) suggest that the forecast uncertainty may be better represented by larger localization scales, and that smaller observation errors in the altimeters may improve the water level forecast. Due to the influence of the nearby fixed stations, the altimeters' impact is somehow masked in this validation.
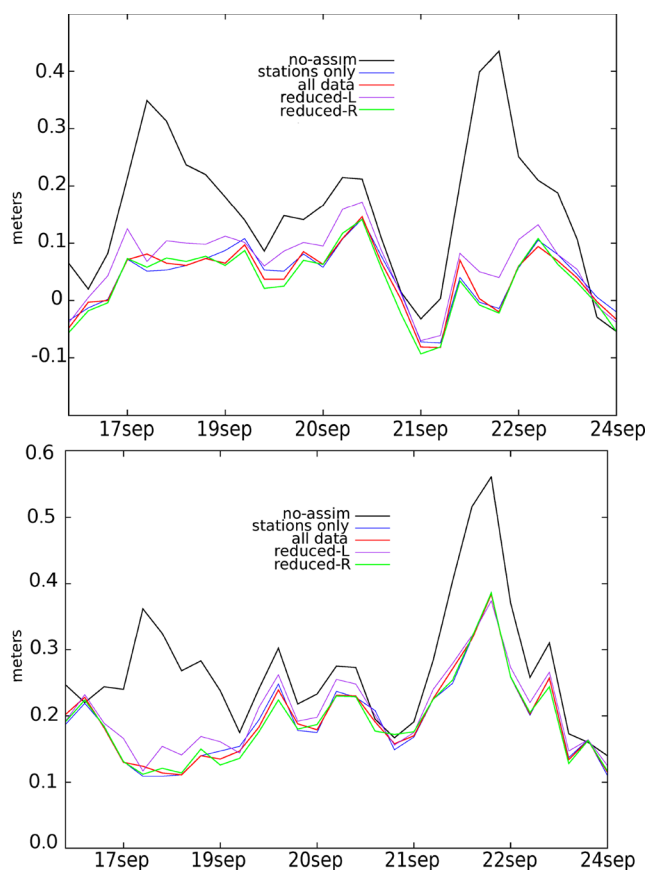

Fig. 9 Mean *(upper)* and standard deviation of the observational departure *(lower panel)* of the very short-range (3 to 9 h) forecast ensemble mean in Atalaya and Santa Teresita during the 17−24 September stormy week. The *black line* denotes the control run without assimilation. Standard localization in *blue* and *red lines* is L=500 km (fixed stations and all data, respectively) and standard observation RMSE=11 cm for altimeters in the *red line*. Reduced RMSE=5 cm *(green)*; a reduced localization scale L=300 km *(purple)* yielded no benefit

6 Conclusions

Through these limited experiments, we have been able to outline a general approach to the joint use of tide gauge and altimeter storm surge observations, available from very recent improvements in coastal altimetry. Although storm surge data assimilation has been assessed and successfully applied on an operational basis (Verlaan et al. 2005), the availability of conventional data and local scenario vary considerably from case to case. We achieved some insight into the importance of a correction in the initial state for the storm surge prediction, given the local morphology and according to the scale of the perturbations, different sources and distribution of data. The isolated effects of some parameters which are significant to the assimilation, such as observational errors, localization scale and additive inflation, have been assessed. We demonstrated the adequacy of the analysis increments produced by this ensemble-based scheme, given the sparse and uneven distribution of altimeter data.

Source of uncertainties in the storm surge forecast are not completely captured by the atmospheric and storm surge model ensembles. More adequate sources have to be identified for the former, in order to advance towards a fully established system. The later should be improved by considering several model uncertainties that have been identified in Etala (2009a, b) in parameterizations and forcing, respectively, during the calibration of the model. The 4D-LETKF from its side provides analysis perturbations in the initialization that are ideally representative of analysis and observational errors. The underestimation of any of these elements would result in an overestimation of the model accuracy, providing an overweighting of the background relatively to observations in the analyses results. The need for adding external perturbations into the ensemble suggests our still incomplete understanding of the system uncertainties.

The events shown provided few but significant examples to test the performance of the 4D-LETKF assimilation scheme applied to the storm surge prediction problem. However, the results from this prototype cannot be considered as representative of the full operational system. Being a deterministic-type EnKF, the scheme introduced for storm surge data assimilation provides an excellent opportunity to further applications in the deterministic model with increased resolution in the forcing fields, in order to explore the impact on longer forecast horizons. As an EnKF, its formulation is independent from the model used, hence, it is subjected to minimal changes upon any model update. Its optimal performance in parallel computing environments due to the local independent calculations makes it one of the most cost-effective advanced methods for data assimilation.

The most important result we obtained in this work was the remarkable positive impact of the data assimilation on the short-range surge prediction at the mid and outer Río de la Plata. The impact at the inner estuary was not tested directly, but can be inferred. The strongest reduction of the error in the forecasted storm surge level was obtained by introducing the assimilation in the forecast cycle. Objective measures derived from differences in parameterization details were negligible when compared with the overall impact of the data assimilation. Satellite altimetry data are very useful in the current scenario. Nevertheless, the value of extra off-shore information could not be fully assessed, due to the absence of real-time data from tide gauges in extensive areas along the Argentine coast.

These preliminary results suggest that numerical prediction of the storm surge on the Argentine coast would benefit from the availability of real-time observations through an advanced assimilation method. We have demonstrated the impact of an improved initial state in the short-range forecast. The magnitude of the impact obtained at the mouth and middle estuary with the assimilation suggests that a significant improvement in the storm surge forecast at the populated head may be achieved, particularly when warning-levels are expected. This ongoing work is a part of a collaborative effort aimed at enhancing operational capabilities at the SHN.

References

Altaf MU, Butler T, Mayo T, Luo X, Dawson C, Heemink AW, Hoteit I (2014) A comparison of ensemble Kalman filters for storm surge assimilation. Mon Weather Rev 142(8):2899–2914

Butler T, Altaf MU, Dawson C, Hoteit I, Luo X, Mayo T (2012) Data assimilation within the advanced circulation (ADCIRC) modeling framework for hurricane storm surge forecasting. Mon Weather Rev 140(7):2215–2231

Cañizares R, Heemink AW, Vested HJ (1998) Application of advanced data assimilation methods for the initialisation of storm surge models. J Hydraul Res 36(4):655–674

Cipollini P, Benveniste J, Bouffard J, Emery W, Fenoglio-Marc L, Gommenginger C, Griffin D, Høyer J, Kurapov A, Madsen K et al (2010) The role of altimetry in coastal observing systems. Proceedings of OceanObs 9

Etala P (2009a) Dynamic issues in the SE South America storm surge modeling. Nat Hazards 51:79–95

Etala P (2009b) On the accuracy of atmospheric forcing for extratropical storm surge prediction. Nat Hazards 51(1):49–61

Evensen G (1994) Sequential data assimilation with a nonlinear quasi-geostrophic model using Monte Carlo methods to forecast error statistics. J Geophys Res 99(C5):10143–10162

Heemink AW, Kloosterhuis H (1990) Data assimilation for non-linear tidal models. Int J Numer Methods Fluids 11(8):1097–1112

Hunt BR, Kostelich EJ, Szunyogh I (2007) Efficient data assimilation for spatiotemporal chaos: a local ensemble transform Kalman filter. Physica D: Nonlinear Phenomena 230(12):112–126

Kalnay E, Li H, Miyoshi T, Yang SC, Ballabrera-Poy J (2007) 4DVar or ensemble Kalman filter? Tellus 59(5 09):758–773

Li Y, Peng S, Yan J, Xie L (2013) On improving storm surge forecasting using an adjoint optimal technique. Ocean Modelling 72:185–197

Lionello P, Sanna A, Elvini E, Mufato R (2006) A data assimilation procedure for operational prediction of storm surge in the northern Adriatic Sea. Cont Shelf Res 26(4):539–553

Miyoshi T, Yamane S (2007) Local ensemble transform Kalman filtering with an AGCM at a T159/L48 resolution. Mon Weather Rev 135(11):3841–3861

Naeije M, Schrama E, Scharroo R (2000) The Radar Altimeter Database System project RADS, Geoscience and Remote Sensing Symposium, IGARSS 2000, IEEE 2000, International, vol 2

Ott E, Hunt BR, Szunyogh I, Zimin AV, Kostelich EJ, Kostelich M, Corazza M, Sauer T, Kalnay E, Patil DJ, Yorke JA (2004) A local ensemble Kalman filter for atmospheric data assimilation. Tellus 56A:415–428

Peng SQ, Xie L (2006) Effect of determining initial conditions by four-dimensional variational data assimilation on storm surge forecasting. Ocean Model 14.1:1–18

Philippart M, Gebraad A, Scharroo R, Roest M, Vollebregt E, Jacobs A, van den Boogaard H, Peters H (1998) Data assimilation with altimetry techniques used in a tidal model, 2nd program. DATUM 2 Project NRSP-2 98-19. Tech. rep., Netherlands Remote Sensing Board (BCRS)

Saraceno M, D'Onofrio EE, Fiore ME, Grismeyer WH (2010) Tide model comparison over the Southwestern Atlantic Shelf. Cont Shelf Res 30(17):1865–1875

van Velzen N, Verlaan M (2007) COSTA a problem solving environment for data assimilation applied for hydrodynamical modelling. Meteorol Z 16(6):777–793

Verlaan M, Heemink AW (1997) Tidal flow forecasting using reduced rank square root filters. Stoch Hydrol Hydraul 11:349–368

Verlaan M, Zijderveld A, de Vries H, Kroos J (2005) Operational storm surge forecasting in the netherlands: developments in the last decade. Phil Trans R Soc A: Math, Phys Eng Sci 363(1831):1441–1453

Wei M, Toth Z, Wobus R, Zhu Y (2008) Initial perturbations based on the ensemble transform (ET) technique in the NCEP global operational forecast system. Tellus 60A:62–79